



Universiteit
Leiden
The Netherlands

Shear stress regulation of endothelial glycocalyx structure is determined by glucobiosynthesis

Wang, G.Q.; Kostidis, S.; Tiemeier, G.L.; Sol, W.M.P.J.; Vries, M.R. de; Giera, M.; ... ; Rabelink, T.J.

Citation

Wang, G. Q., Kostidis, S., Tiemeier, G. L., Sol, W. M. P. J., Vries, M. R. de, Giera, M., ... Rabelink, T. J. (2020). Shear stress regulation of endothelial glycocalyx structure is determined by glucobiosynthesis. *Arteriosclerosis, Thrombosis, And Vascular Biology*, 40(2), 350-364.
doi:10.1161/ATVBAHA.119.313399

Version: Publisher's Version
License: [Creative Commons CC BY 4.0 license](https://creativecommons.org/licenses/by/4.0/)
Downloaded from: <https://hdl.handle.net/1887/3181570>

Note: To cite this publication please use the final published version (if applicable).

BASIC SCIENCES

Shear Stress Regulation of Endothelial Glycocalyx Structure Is Determined by Glucobiosynthesis

Gangqi Wang, Sarantos Kostidis, Gesa L. Tiemeier, Wendy M.P.J. Sol, Margreet R. de Vries, Martin Giera, Peter Carmeliet, Bernard M. van den Berg, Ton J. Rabelink

OBJECTIVE: Endothelial cells exposed to laminar shear stress express a thick glycocalyx on their surface that plays an important role in reducing vascular permeability and endothelial anti-inflammatory, antithrombotic, and antiangiogenic properties. Production and maintenance of this glycocalyx layer is dependent on cellular carbohydrate synthesis, but its regulation is still unknown.

APPROACH AND RESULTS: Here, we show that biosynthesis of the major structural component of the endothelial glycocalyx, hyaluronan, is regulated by shear. Both in vitro as well as in vivo, hyaluronan expression on the endothelial surface is increased on laminar shear and reduced when exposed to oscillatory flow, which is regulated by KLF2 (Krüppel-like Factor 2). Using a CRISPR-CAS9 edited small tetracysteine tag to endogenous HAS2 (hyaluronan synthase 2), we demonstrated increased translocation of HAS2 to the endothelial cell membrane during laminar shear. Hyaluronan production by HAS2 was shown to be further driven by availability of the hyaluronan substrates UDP-glucosamine and UDP-glucuronic acid. KLF2 inhibits endothelial glycolysis and allows for glucose intermediates to shuttle into the hexosamine- and glucuronic acid biosynthesis pathways, as measured using nuclear magnetic resonance analysis in combination with ¹³C-labeled glucose.

CONCLUSIONS: These data demonstrate how endothelial glycocalyx function and functional adaptation to shear is coupled to KLF2-mediated regulation of endothelial glycolysis.

VISUAL OVERVIEW: An online [visual overview](#) is available for this article.

Key Words: cell membrane ■ endothelial cells ■ glucose ■ metabolism ■ UDP-glucosamine ■ UDP-glucuronic acid

The endothelium is covered by a glycocalyx surface layer, which consists of the polysaccharides heparan sulfate, hyaluronan, and chondroitin sulfate.^{1,2} This layer confers most of the functional aspects of the endothelium. For example, specific sulfation patterns on heparan have been shown to be critical for engagement of growth factors and chemokines to their receptors and the function of surface-bound proteins such as complement factor H and antithrombin III. In addition, this layer serves as barrier that governs capillary ultrafiltration. Finally, the glycocalyx layer transmits the shear forces of the flowing blood to the intracellular pathways that induce endothelial quiescence, such as KLF2 (Krüppel-like factor 2). Conversely, altered shear forces have also been associated with changes in glycocalyx thickness.^{3,4}

How the glycocalyx is synthesized and maintained to keep the endothelium in its quiescent state is unknown.

The main structural component of the endothelial glycocalyx is hyaluronan (HA). HA is a very long polysaccharide that is synthesized at the inner surface of the plasma membrane from the substrates UDP-glucosamine (UDP-GlcNAc) and UDP-glucuronic acid (UDP-GlcA). HA is synthesized by the synthases HAS1 (hyaluronan synthase 1), HAS2 (hyaluronan synthase 2), or HAS3 (hyaluronan synthase 3) and secreted into the extracellular space. These 3 isoforms differ in enzyme stability, elongation rate of HA, and affinity of HA substrates,⁵ which potentially influences HA synthesis. HAS2 is the most widespread isoform correlated with HA distribution in mammals.⁶ HAS2 knockout mice die early in gestation due to major

Correspondence to: Ton J. Rabelink, MD, PhD, Division of Nephrology, Department of Medicine, Einthoven Laboratory for Experimental Vascular Research, Leiden University Medical Center, Albinusdreef 2, 2333 ZA, Leiden, the Netherlands. Email aj.rabelink@lumc.nl

The online-only Data Supplement is available with this article at <https://www.ahajournals.org/doi/suppl/10.1161/ATVBAHA.119.313399>.

For Sources of Funding and Disclosures, see page 363.

© 2019 American Heart Association, Inc.

Arterioscler Thromb Vasc Biol is available at www.ahajournals.org/journal/atvb

Nonstandard Abbreviations and Acronyms

HA	hyaluronan
HAS1	hyaluronan synthase 1
HAS2	hyaluronan synthase 2
HAS3	hyaluronan synthase 3
HFD	high-fat diet
HUVEC	human umbilical vein endothelial cell
KLF2	Krüppel-like factor 2
NMR	nuclear magnetic resonance
PFKFB3	6-phosphofructo-2-kinase/fructose-2,6-biphosphatase 3
TNF	tumor necrosis factor
UDP-Glc	UDP glucose
UDP-GlcA	UDP glucuronic acid
UDP-GlcNAc	UDP-N-acetylglucosamine

defects in cardiovascular development, suggesting that HA may function as molecular platform for vascular signaling.⁷ It is estimated that HAS2 polymerizes UDP-GlcA and UDP-GlcNAc at a rate of 20 monosaccharides/s,⁵ rendering the synthesis critically dependent upon the cytosolic availability of these substrates.

UDP-GlcA and UDP-GlcNAc are derived from respectively the glucuronic acid and hexosamine biosynthesis pathways. We therefore postulated that endothelial HA, and hence glycocalyx thickness, would depend upon endothelial glucose metabolism. It has been shown that, in this respect, endothelial cells are characterized by a high glycolytic flux, where the possibility for glucobiosynthesis can be postulated to be regulated by this flux. Interestingly, the shear stress responsive transcription factor KLF2 has been shown to inhibit PFKFB3 (6-Phosphofructo-2-Kinase/Fructose-2,6-Biphosphatase 3),⁸ the key enzyme that drives (hyper)glycolysis.

In this study, we investigate the relationship and interdependency of shear adaptation, glucobiosynthesis, and the ability to synthesize the glycocalyx layer, which is so critical for endothelial function.

MATERIAL AND METHODS

The authors declare that all supporting data are available within the article and in the [online-only Data Supplement](#).

Mice and Experimental Groups

The details of the mice experiment has been described previously.⁹ Given the implications found that sex differences exist in relation to volume regulation and exchange vascular homeostasis,¹⁰ only male mice were taken in this study to decrease the outcome variability. In brief, all experiments were performed using 8-week-old male (apoE^{-/-}) mice on C57BL/6J background (Charles River), randomly divided into 4 groups. One group was fed a standard rodent diet (NC; Sniff R/M-H,

Highlights

- Quiescent endothelial cells, induced by prolonged laminar shear stress, presented a thicker glycocalyx hyaluronan on the surface.
- Laminar shear stress induces endothelial hyaluronan production through KLF2 (Krüppel-like factor 2) regulated HAS2 (hyaluronan synthase 2) expression and UDP-sugar availability.
- Endothelial cells need proper amount of hyaluronan to keep its integrity, which is determined by the metabolic state of endothelial cells.

Germany) for 6 weeks (n=6). The other 3 groups of mice were put on a high fat-, high-cholesterol diet containing 15% cacao butter, 0.25% cholesterol, 40.5% sucrose, 10% corn starch, 1% corn oil, and 5.95% cellulose (high-fat diet; diet-W, Hope farms, the Netherlands) for 6 weeks. At the age of 14 weeks, 2 of the groups on high-fat diet received an osmotic minipump and mouse jugular catheter (Alzet, Cupertino, CA) containing active- (n=6) or inactive (n=7) testicular hyaluronidase (bovine testis, Sigma-Aldrich). The mice were sacrificed under anesthesia. All the mice were kept with ad libitum food and water in cages with bedding (Rehohix Corncob bedding MK1500, Technilab-BMI, Someren, the Netherlands) in a 12/12 hours light/dark cycle. The experimental protocol was approved by the local Animal Ethical Committee of Maastricht University (AEC protocol number 2007-031), and all animal work was performed in compliance with the Dutch government guidelines.

Cell Isolation and Culture

Human umbilical vein endothelial cells (HUVECs) were freshly isolated, by perfusion and subsequent incubation (20 minutes) of trypsin at 37°C, from different donors as described¹¹ (with approval of the Medical Ethical Commission of the Leiden University Medical Center, and informed consent from all subjects) and used between passage 1 and 3. Freshly isolated HUVECs were cultured in 0.1% gelatine-coated plastic flasks in endothelial EGM2 (Lonza) medium, supplemented with human epidermal growth factor, vascular endothelial growth factor, human fibroblast growth factor-B, R3-IGF-I, ascorbic acid, heparin, and 10% human serum (CC-3121; Lonza, Basel, Switzerland), and with antibiotics/antimycotics (Life technology, Gibco), at 37°C and 5% CO₂. HUVECs were treated with 1 mmol/L UDP-GlcA (Sigma, U6751), 1 mmol/L UDP-GlcNAc (Sigma, U4375), or 10 μmol/L 3PO (Merck, 525330) for 72 hours, or treated with 100 μmol/L 2DG (Sigma, D8375) for 24 hours. Cells were collected for further experimental assays.

In Vitro Flow Experiments

HUVECs were cultured for 4 days at a constant laminar shear stress (10 dyne/cm²) or an oscillatory shear stress (±10 dyne/cm²; 0.5 Hz) in EGM2 (Lonza) using an ibidi flow system (Ibidi, Martinsried, Germany). Medium was refreshed after 1 day, nonadhered cells removed, and cultured under laminar or oscillatory flow for another 3 days at 37°C and 5% CO₂. To test the effects of laminar versus oscillatory shear patterns, we used the same shear stress level of 10 dyne/

cm² exposure for both the laminar- and the oscillatory flow groups. Shear stress levels *in vivo* have been reported to range from 2 to 16 dyne/cm².¹² While initial reports reported oscillatory shear to be possibly lower,¹³ it was later confirmed to be also around 10 dyne/cm², and consequently this range is currently widely used in *in vitro* experimental setups to study the response of disturbed shear.^{14–18}

Neurocan-dsRed Construct

The N-terminus rat neurocan construct of the HA specific neurocan-eGFP (enhanced green fluorescent protein; Ncan-eGFP) construct,¹⁹ linked to the BM 40 signal peptide with APLGRGSHHHHHGGLA and a GSSGA linker at the C-terminus, was excised and fused into a pDsRedMonoN1 (ClonTech, Mountain View, CA) plasmid. The modified neurocan-dsRed (Ncan-dsRed) construct was incorporated into a self-inactivating lentiviral vector (pLV-CMV-IE.NcandRed) and transduced into Hek293 cells. Supernatant was isolated and purified on a Ni-NTA resin column using the incorporated 6×Histidine tag within the protein.

Glycocalyx and HA Staining

Deparaffinized mouse aorta sections (4-μm thick) were washed in PBS and antigen retrieval was performed in a citrate (pH 6.0) buffer in an autoclave. Slides were blocked in Serum-Free Protein Block buffer (Dako, Agilent Technologies Netherlands B.V., Amstelveen, the Netherlands) for 1 hour at room temperature. Ncan-dsRed was incubated overnight (at 4°C) in HBSS (Gibco, 14175-053), followed by washing with HBSS and embedded in Prolong gold antifade mountant with DAPI (ThermoFisher, P36931).

Cells were fixed with 4% PFA in HBSS for 10 minutes at room temperature, washed in HBSS containing 1% BSA, and blocked for 30 minutes at room temperature in 5% BSA in HBSS. Ncan-dsRed or 10 μg/mL lectin from *Lycopersicon esculentum* (Sigma-Aldrich, L0401) were incubated overnight (at 4°C) together with Hoechst 33258 (Invitrogen, H3569), followed by wash with 1% BSA in HBSS. Cells were examined using a LEICA TCS SP5 with a 100× objective (HCX PL APO CS 100×/1.40 oil, Leica). Sequential 16-bit confocal images (xyz dimensions, 0.142×0.142×0.3 μm, 0.142×0.142×1 μm, or 0.116×0.116×1 μm) were recorded using LAS-X Image software (Leica) and analyzed with ImageJ. Surface glycocalyx and HA expression was quantified on 5 cells per field of view of 4 independent experiments, in essence as described earlier.²⁰ From a side view, resliced from a line (10 pixels wide) over the nucleus 3 additional lines were drawn at the nuclear position, and the mean fluorescence was calculated between the distance from half-maximum signal of the nuclear staining to half-maximum signal at the luminal end. Both thickness and average fluorescence were determined.

Immunofluorescence Staining

Deparaffinized mouse aorta sections (4 μm thick) were washed in PBS, and antigen retrieval was performed in a citrate (pH 6.0) buffer in an autoclave. Slides were blocked with 3% normal goat serum, 2% BSA, and 0.01% Triton-X100 in PBS for 1 hour at room temperature. Primary anti-KLF2 antibody (abcam,

ab203591), anti-mouse ICAM1 (Santa Cruz, sc-1511r), or rabbit IgG isotype control (abcam, ab172730) was incubated overnight (at 4°C), followed by Goat anti rabbit IgG AF488 for 1 hour. Slides were embedded in Prolong gold antifade mountant with DAPI (ThermoFisher, P36931).

Cells were fixed with 4% PFA in PBS for 10 minutes at room temperature, washed with PBS, and blocked for 1 hour at room temperature in block buffer (3% normal goat serum, 2% BSA, and 0.3% triton in PBS). Anti-human CD144 (BD bioscience, 6273648), Phalloidin-Tetramethylrhodamine B isothiocyanate (Sigma, P1951), and Hoechst 33258 (Invitrogen, H3569) were incubated overnight (at 4°C), followed by wash with PBS; then, incubated with Goat anti mouse IgG1 AF488 for 1 hour at room temperature and washed with PBS.

RNA Isolation and RT-PCR

Cells were harvested in Trizol reagent (Life Technologies, 1559601,8). Total RNA was isolated using RNeasy mini kit (Qiagen, 74106) according to its protocol. cDNA was synthesized by mixing 1 mg total RNA, Oligo (dT; Promega, C110A), and dNTP (Promega, C110A) and incubated at 65°C for 5 minutes first. Then M-MLV reverse transcriptase (Promega, M170B), recombinant RNasin ribonuclease inhibitor (Promega, N251B), and DTT were added into the mixture and incubated at 37°C for 50 minutes. The reaction was terminated by incubating at 70°C for 15 minutes. SYBR select master mix (Applied Biosystems, 4472897) and specific primers (Table I in the [online-only Data Supplement](#)) was used for real-time PCR. The expression of genes were determined by normalized to GAPDH levels.

Virus Transduction

The HAS2 and HAS3 short-hairpin RNA lentiviral constructs (pLV-CMV-IE.HAS2shRNA, pLV-CMV-IE.HAS3shRNA) were created through transfecting Hek293 cells (20%–40% confluence) with a mixture of combined plasmid DNA of Has2shRNA (Sigma-Aldrich, Mission shRNA library #9868) or Has3shRNA (Sigma-Aldrich, Mission shRNA library #9903), H1/VSVG and H23/pspax2 with polyethylenimine (PEI, 0.05 mg/mL final concentration) in DMEM (Gibco) to obtain the self-inactivating lentiviral construct from supernatant, in principle as described.²¹ Primary HUVECs were cultured to 60% to 80% confluency in T75 flasks (Greiner bio-one, Alphen a/d Rijn, the Netherlands) in EGM2 medium and transduced with pLV-CMV-IE.HAS2shRNA, HAS3shRNA, or control (pLV-CMV-IE) in combination with 8 μg/mL polybrene, incubated o/n at 37°C and 5% CO₂. After medium refreshment, incubated for another 48 hours before collecting for experimental assays.

To induce a transient constitutive high expression of HAS2 and production of HA, the human *HAS2/pIRES-2-eGFP*²² construct (gift from J.B. McCarthy) was transferred into pShuttleCMV-Luciferase to create the adenoviral vector Ad5CMV-HAS2, adenoviral control is Ad5CMV-Luciferase.²³ For infection of HUVECs with the adenoviral constructs, cells were cultured to 60% to 80% confluency. Two multiplicity of infection virus in combination with 8 μg/mL polybrene in EGM2 medium were added into the cells and incubated o/n at 37°C and 5% CO₂. After medium refreshment, incubated for another 24 hours before collecting for experimental assays.

Glycolytic Flux Measurement

HUVECs were seeded overnight at 6×10^4 cells per well on fibronectin (Sigma) coated Seahorse XF96 polystyrene tissue culture plates (Seahorse Bioscience). The plate was incubated in unbuffered DMEM assay medium (Sigma) for 1 hour in a non-CO₂ incubator at 37°C before measuring in an XFe 96 extracellular flux analyser (Seahorse Bioscience). Extracellular acidification rate was measured over 4-minute periods with a mixing of 2 minutes in each cycle, with 5 cycles in total. Inhibitors and activators were used at the following concentrations: glucose (5 mmol/L), oligomycin (5 μmol/L), and 2-DG (100 mmol/L). Cellular protein content was determined with a BCA-protein kit from Pierce (Thermo-Fischer Scientific), and the data were represented as extracellular acidification rate normalized to protein.

Metabolites Measurement

Quantitative analysis of intracellular and extracellular metabolites in *in vitro* EC cultures was performed using nuclear magnetic resonance (NMR) spectroscopy as described in detail elsewhere.^{24,25} Briefly, MOCK and *KLF2^{OE}* ECs in triplicates were washed with warm PBS (37°C) to remove the culture medium and quickly quenched with liquid nitrogen to arrest metabolism. The cells were subsequently scraped of the plates and extracted using a cold (−80°C) solution of methanol/chloroform/water, 8.1:0.9:1 (v/v/v). After leaving the samples on dry ice for 30 minutes, the extracts were centrifuged for 20 minutes at 18000×g, at 4°C.

Before washing ECs with PBS, 0.2 mL of culture medium was collected from each sample and mixed with 0.4 mL of cold (−80°C) 100% LC-grade methanol to extract extracellular metabolites. All samples were subsequently placed at −80°C for at least 30 minutes and centrifuged for 20 minutes at 18000×g, at 4°C.

The supernatants from both cell extracts and culture medium extracts were collected and dried with nitrogen gas. NMR samples of extracts were prepared by dissolving the dried material with 0.22 mL of 0.15 M phosphate buffer (pH 7.4) in deuterated water containing 0.05 mmol/L trimethylsilyl propionic-d₄-sodium salt (TSP-d₄) as internal standard for NMR referencing and quantification. A 1D ¹H-NMR spectrum was collected for each sample on a 14.1 T (600 MHz for ¹H) Bruker Avance II NMR, using the 1D-NOESY experiment with pre-saturation as implemented in the spectrometer library (Topspin v3.0, pulse sequence: *noesygppr1d*; Bruker Biospin, Ltd). All spectra were processed to correct the phase and baseline and imported in Chenomx NMR suite 8.4 (Chenomx NMR suite, v8.0, Edmonton, Canada) for quantification of metabolites. The protein bullet was dissolved in lysis buffer (150 mmol/L NaCl, 1% SDS, 0.5% deoxycholate, and 0.5% triton X-100, pH 7.5) with sonification. The protein concentration was measured using Pierce BCA protein assay kit (ThermoFisher, 23225) according to its manual. All concentrations were normalized to the total protein mass of each sample.

For ¹³C fractional enrichment analysis, triplicates of MOCK and *KLF2^{OE}* were cultured in glucose-free medium, enriched by 5 mmol/L U-¹³C₆-D-glucose and processed as described above. Fractional enrichment was calculated as described elsewhere²⁵ by deconvoluting and quantifying the protons at 5.52, 5.60, and 5.62 ppm (from UDP-GlcNAc, UDP-Glc, and

UDP-GlcA, respectively), the protons at 5.99 to 6.03 ppm (overlapped peaks from all 3 sugars) and the protons at 7.9 ppm (overlapped peaks from all 3 sugars).

HA Size Analysis

For HA size analysis, we used the online protocol from Cleveland Clinics (NHLBI # PO1HL107147). HUVECs were digested with proteinase K solution (0.1 mg/mL proteinase K [Promega, V302B], 0.001% SDS, 100 mmol/L ammonium acetate, pH 7.0) for 4 hours at 60°C. Samples were precipitated and washed with cold ethanol. Nucleic acid was digested with benzonase nuclease (Sigma, E1014) at 60°C overnight and enzyme was inactivated in a boiling water bath for 5 minutes. Samples were precipitated and washed with cold ethanol again. Samples were resuspended in 10 M formamide and loaded in a 0.5 cm thick 1% agarose gel and run for 1.5 hours. Finally, the gel was stained with stain-all (Sigma, E9379) solution and imaged with a camera.

CRISPR Cas9 Editing

Experiments were performed using the Alt-R CRISPR-Cas9 system (Integrated DNA technologies, IDT) according to manufacturers' user guide. Guide RNA (gRNA, TGACTGCAAACGTCAAAACATGG) specific targeted to the HAS2 c-terminal was designed and gRNA containing crRNA was synthesised by IDT. A crRNA:tracrRNA duplex was formed by incubating 2 synthetic modified RNAs (crRNA and tracrRNA) at 95°C for 5 minutes. Ribonucleoprotein complexes were formed by incubating crRNA:tracrRNA duplex and Alt-R S.p. Cas9 nuclease (IDT, 1081060) at room temperature for 20 minutes. A single-stranded oligodeoxynucleotide repair template contained a small tetracysteine tag (TC-tag, Cys-Cys-Pro-Gly-Cys-Cys, GGACAACAAT ATG ACATG GTGCTT GAT GTATGTT GT CCTGGC TGTTGTT GATCTTCTATGTT TTGAC GTTTGCAGTC ACACACAAC ACC TT) was synthesised by IDT. Ribonucleoprotein complexes and single-stranded oligodeoxynucleotide were co-delivered into HUVECs using Amaxa HUVEC nucleofactor kit (Lonza, VPB-1002) according to its manual.

HAS2-TC Imaging

Cells were gently washed with prewarmed (37°C) HBSS and immersed with 2 μmol/L FIAsh-EDT₂ (Cayman, 20704) in prewarmed HBSS and 10 μmol/L 1,2-ethanedithiol (EDT) at 37°C for 30 minutes. Aspirate FIAsh-EDT₂ solution from cells and replaced with 250 μmol/L 2,3-dimercaptopropanol (BAL) in HBSS at 37°C for 15 minutes. Wash solution was removed and replaced with prewarmed HBSS. HAS2-TC-positive cells were imaged on a LEICA SP8 WLL confocal microscope. Sequential 16-bit confocal images (xyz dimensions, 0.142×0.142×0.3 μm) were recorded and 3-dimensional images were rendered using LAS-X Image software (Leica). The total stained area of each cell was analyzed using ImageJ software.

Immunoblotting

Western blots were performed from protein extracts of HUVECS. Cells were washed with PBS and lysed in 50 mmol/L Tris-HCL buffer (pH 7.5) containing 150 mmol/L NaCl, 1% SDS, 0.5% deoxycholate, and 0.5% triton X-100. Protein samples were diluted 5× in SDS sample buffer (pH 6.8; 10% SDS, 25% 2-mercaptoethanol, 50% glycerol, 0.01% bromophenol

blue, 0.3125M Tris-HCl, 0.5M DTT), incubated at 95°C for 10 minutes, and subjected to SDS-PAGE and Western blotting. Proteins, transferred to PVDF membrane (1704156, Bio-Rad Laboratories BV, Veenendaal, the Netherlands) were detected with antibodies against GAPDH (MA5-15738, ThermoFisher) and ICAM1 (4915s, Cell signaling technology), after blocking the membrane with 5% fat-free milk in PBS and 0.1% Tween-20. Followed by incubation with a secondary HRP-conjugated antibody and Pierce ECL Western Blotting substrate (32106, Thermo Scientific). Band intensity was analyzed using ImageJ software. For the HAS2 protein expression detection, protein samples together with antibodies against HAS2 (sc-34067, Santa Cruz) or GAPDH (MA5-15738, ThermoFisher) were applied in WES machine (Proteinsimplex, CA). The protein expression was measured based on the intensity of peaks given by WES, and a representative digital band was shown.

Statistical Analysis

Data are presented as mean±SD, unless indicated otherwise. For all experiments, 3 to 5 biological replicates were performed. All data were performed with Shapiro-Wilk test and Levene test to evaluate the normality and variances first. For the normally distributed and equal variance data, the differences between 2 groups were assessed by paired 2-tailed Student *t* test and between multiple groups were assessed by 1-way ANOVA followed by Tukey test. $P < 0.05$ were considered statistically significant. If the data were not normally distributed or not of equal variance, the Mann-Whitney *U* test was performed. $P < 0.05$ were considered statistically significant.

RESULTS

Laminar Shear Stress Induces Surface HA Production Through Increased HAS2 Expression

Shear stress plays a crucial role in glycocalyx modeling and endothelial integrity. To test the glycocalyx HA expression upon the atheroprotective- or atheroprone shear stress in vivo, a specific HA-binding peptide (Ncan-dsRed) was used to stain HA in mouse aorta. Endothelial cells exposed to laminar shear stress showed a higher HA expression than the endothelial cells at lesion prone sites exposed to disturbed shear stress in apoE-KO mouse aorta, which revealed a higher ICAM1 expression (Figure 1A through 1D). To explore the role of endothelial HA in the progress of atherosclerosis, ApoE-KO mice at a high-fat diet were studied. At the lesion sites exposed to disturbed shear stress, endothelial HA was diminished and instead increased ICAM1 expression was observed (Figure 1A through 1C in the [online-only Data Supplement](#)). Furthermore, endothelial HA removal by chronic infusion with active hyaluronidase in ApoE-KO mice on high-fat diet (Figure 1D and 1E in the [online-only Data Supplement](#)) showed further loss of HA in

the disturbed shear stress region and resulted in formation of advanced lesions with increased matrix deposition.⁹ Also, in the laminar shear stress regions, increased ICAM1 expression was observed (Figure 1F and 1G in the [online-only Data Supplement](#)), which suggested that endothelial cells are activated after loss of luminal surface HA despite the presence of laminar shear.

An Ibidi flow system was also used to culture endothelial cells in vitro. As reported earlier,²⁶ we observed that prolonged laminar shear stress (4–7 days at 10 dyne/cm²) exposure aligned HUVECs into the direction of flow, increased localization of VE-cadherin at the cell borders, and decreased F-actin stress fibers (Figure 1IA in the [online-only Data Supplement](#)). We next tested the luminal glycocalyx layer expression of ECs in response to shear stress. Four days of exposure to 10 dyne/cm² laminar shear stress induces a maximum total intensity of lectin from *L. esculentum* binding, which is significantly increased in comparison to static culture or 4 days of oscillatory shear (Figure 1IB and 1IC in the [online-only Data Supplement](#)). In addition, increased endothelial surface HA expression was also found after 4 days of laminar shear, in comparison to exposure of oscillatory shear or static cultured EC, when stained with Ncan-dsRed (Figure 1E through 1G; Figure 1ID through 1IF in the [online-only Data Supplement](#)). In line with the observed HA production, laminar shear stress induced HAS2 protein expression (Figure 1H and 1I). Gene expression analysis revealed that exposure to prolonged laminar shear increased *HAS2* (Figure 1J) while *HAS3* was decreased (Figure 1K), *HAS1* expression was undetectable (data not shown).

To further corroborate the requirement of HAS2 in endothelial HA production, we cultured HUVECs after silencing *HAS2* or *HAS3* gene expression with a lentiviral shRNA construct (Figure 1IIA in the [online-only Data Supplement](#)). Although normal *HAS2* gene expression was lower than *HAS3* in static cultured HUVECs, only silencing of *HAS2* (*shHAS2*) significantly decreased surface HA expression, -production, and -HMW HA content, while *shHAS3* had no effect (Figure 1IIB through 1IID in the [online-only Data Supplement](#)). Moreover, *shHAS2* blocked the laminar shear stress induced atheroprotective role by increasing *ICAM1* expression (Figure 1IL through 1IN) and decreasing *NOS3* expression (Figure 1O). Overexpression of *HAS2* (*HAS2^{OE}*), in turn, resulted in a strong increase of cellular HMW HA content and surface HA (Figure 1IID through 1IIF in the [online-only Data Supplement](#)). However, *HAS2^{OE}* also increased LMW HA content (Figure 1IID in the [online-only Data Supplement](#)) and intracellular HA production (Figure 1IIE in the [online-only Data Supplement](#)), both possible proinflammatory factors.^{27,28} These data suggest a strict regulation of endothelial HA production to keep cellular integrity.

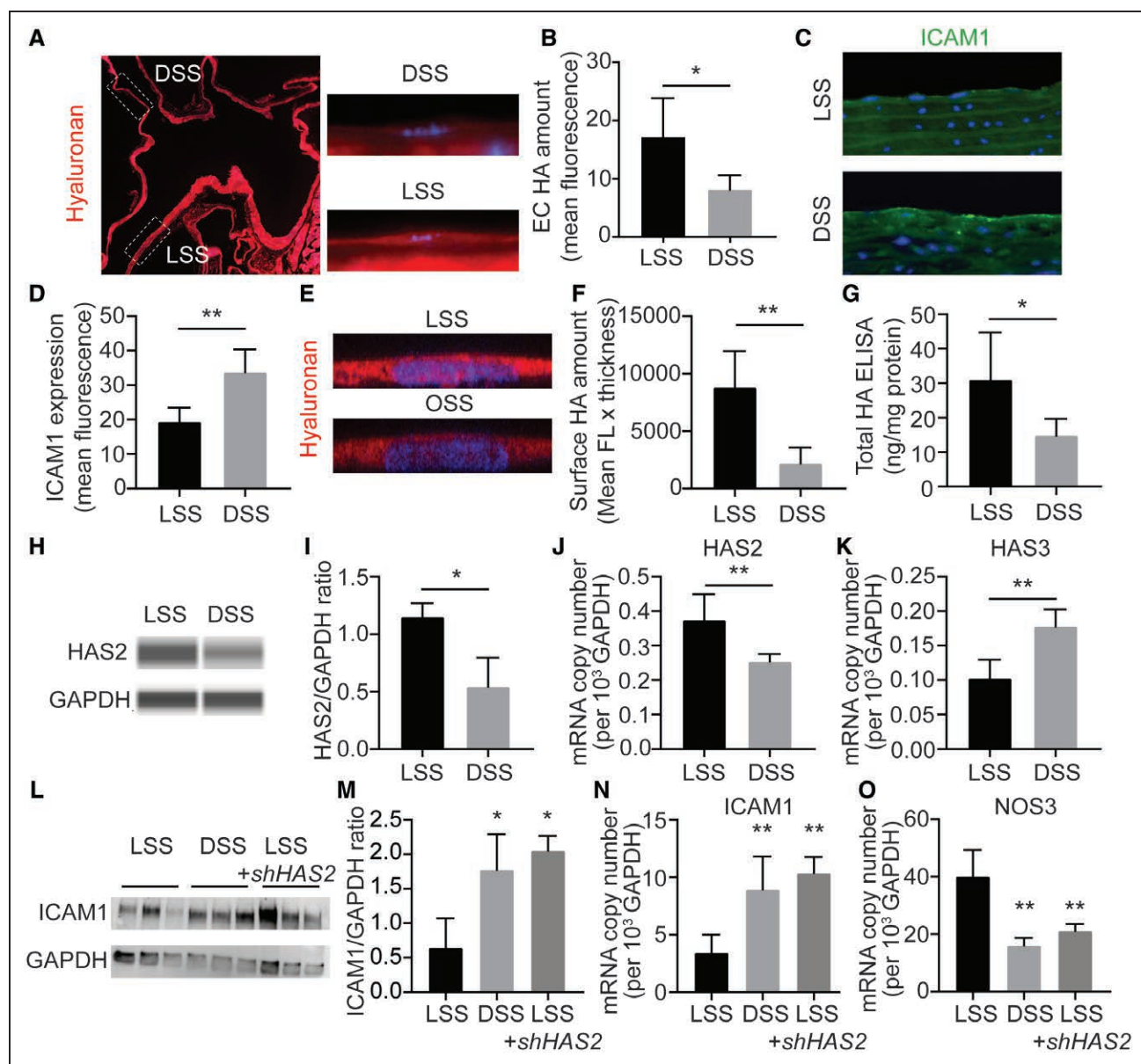


Figure 1. Lamellar shear stress is associated with increased endothelial hyaluronan (HA) and HAS2 (hyaluronan synthase 2) expression.

A, Representative images of HA stained at the surface within the aortic arch region of *apoE*-KO mice on standard diet ($n=6$). Areas exposed to laminar shear stress (LSS) or disturbed shear stress (DSS) are labeled with Ncan-dsRed and demonstrated preferential luminal presence of HA in LSS exposed regions. **B**, Quantification of HA staining in LSS and DSS exposed aortic regions. **C**, Representative images of ICAM1 staining of the aortic regions exposed to LSS and DSS and **(D)** quantification. **E**, Representative confocal images of HA staining of human umbilical vein endothelial cells (HUVECs) after 4 days LSS, or after 4 days exposure to oscillatory shear stress (OSS), respectively. **F**, Quantification of endothelial surface HA under different culture conditions, presented as mean fluorescence times thickness (mean FL \times thickness). **G**, Quantification of total endothelial HA sequence. **H**, Representative WB images of endothelial HAS2 protein expression and **(I)** quantification. **J**, HAS2- and **(K)** HAS3 mRNA expression in response to LSS or OSS, normalized to 10^3 copies GAPDH. **(L)** WB images of ICAM1 protein expression and **(M)** quantification in HUVECs after knockdown of HAS2 (*shHAS2*) or mock virus as control after 4 days of LSS or OSS exposure. **N**, ICAM1- and **(K)** NOS3 mRNA expression under different culture conditions, normalized to 10^3 copies GAPDH. All values are given as mean \pm SD of 3 to 7 independent experiments. Nonpaired 2-tailed Student *t* test and 1-way ANOVA followed by Tukey test were performed; * $P<0.05$, ** $P<0.01$.

Shear Stress Induces HAS2 Protein Amount and Translocation to the Endothelial Apical Membrane

HA is synthesized by its synthases at the inner face of the plasma membrane and secreted into the extracellular

space. To detect the expression and location of HAS2 protein under shear stress, we inserted a small TC-tag (Cys-Cys-Pro-Gly-Cys-Cys) into the C-terminal end of the HAS2 gene (Figure 2A), using codelivery of Cas9 protein precomplexed with 2 synthetic modified RNAs (crRNA and tracrRNA) and a single-stranded oligodeoxynucleotide

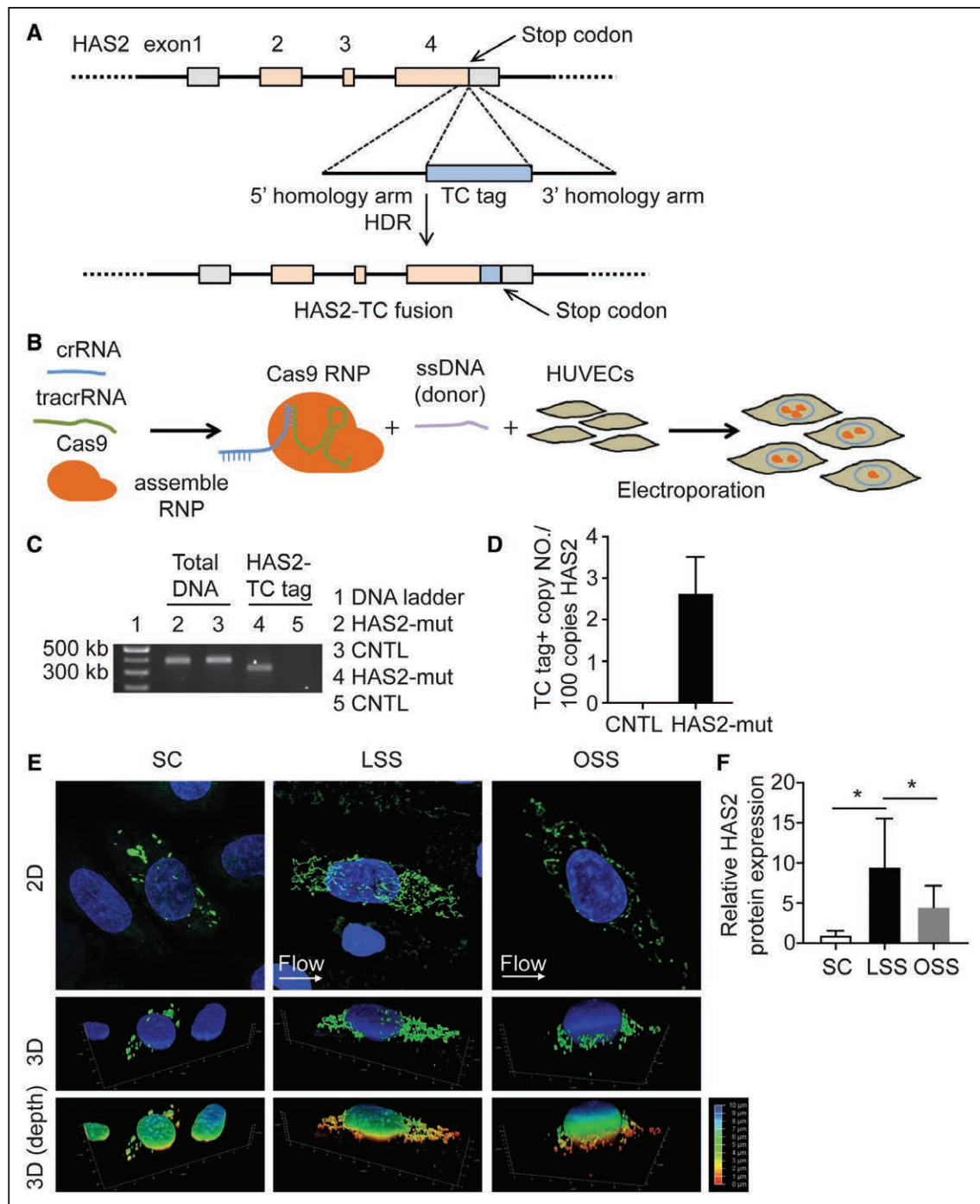


Figure 2. Laminar shear stress induces HAS2 (hyaluronan synthase 2) protein amount and translocation to the endothelial apical membrane.

A, A small tetracycline tag (TC-tag, Cys-Cys-Pro-Gly-Cys-Cys) was inserted into the C-terminal end of the *HAS2* gene using **(B)** codelivery of Cas9 protein precomplexed with 2 synthetic modified RNAs (crRNA and tracrRNA) and a single-stranded oligodeoxynucleotide (ssODN) repair template in human umbilical vein endothelial cell (HUVEC). **C**, Identification of the *HAS2*-TC-tag fusion using PCR and determination of **(D)** efficiency of the knock-in. **E**, Representative images of HAS2-TC-tag protein expression in static culture (SC), laminar shear stress (LSS), and oscillatory shear stress (OSS). HAS2-TC tag visualized in 2-dimensional (top row), 3-dimensional (3D; middle row), and 3D (depth color coding; bottom row). **F**, Quantification of HAS2-TC-tag protein expression, presented as relative to static culture. A total of 12 cells from each group were imaged and quantified. All values are given as mean \pm SD. Nonpaired 2-tailed Student *t* test and 1-way ANOVA followed by Tukey test were performed; **P*<0.05.

repair template in HUVEC (Figure 2B). After conformation of the knock-in (Figure 2C; Figure IVA in the [online-only Data Supplement](#)), the efficiency was determined to

be about 2.5% without selection (Figure 2D). Static EC cultures revealed a low amount of intracellular TC-tagged HAS2 protein after introducing FIAsH-EDT2 labeling

reagent (Figure 2E), while TGF β treatment, as a positive control, induced HAS2 expression (Figure IVB and IVC in the [online-only Data Supplement](#)). When endothelial cells are exposed to laminar shear stress for 4 days, not only the intracellular amount of HAS2 protein increases but translocation of HAS2 to the apical membrane could also be observed compared with exposure to oscillatory shear stress or static culture (Figure 2E and 2F).

Endothelial Krüppel-Like Factor 2 Increases Surface HA Expression

Endothelial cells exposed to laminar shear stress showed a higher KLF2 expression than exposure to disturbed shear stress in mouse aorta (Figure 3A and 3B). In vitro, only prolonged laminar shear stress induces endothelial KLF2 gene expression (Figure 3C). A highly conserved KLF2-binding domain CACCC box^{29,30} was found in the *HAS2* promoter region (Figure 3D), which is a potentially transcriptional regulator of *HAS2* expression. To test a possible link between endothelial *KLF2* expression and HA production, we used a lentiviral *KLF2* construct to increase *KLF2* (*KLF2^{OE}*) in HUVECs. As expected, *KLF2^{OE}* significantly increased both *HAS2* mRNA and protein expression (Figure 3E through 3G). In line with laminar shear stress exposure, *KLF2* overexpression also resulted in increased HA expression (Figure 3H and 3I; Figure VA in the [online-only Data Supplement](#)). Moreover, inhibition of *KLF2* expression blocked the laminar shear stress induced *HAS2* expression and HA production (Figure 3J through 3M).

HAS2 Responsible HA Synthesis in Endothelial Cells Is Dependent on Substrate Availability

In contrast to synthesis of the other glycosaminoglycans, which takes place in the Golgi system, HA is produced at the plasma membrane using the cytoplasmic substrate pool. Therefore, cytosolic availability of UDP-GlcA and UDP-GlcNAc can be postulated to be critical for this process, rendering the metabolic state of the cell an important factor for production of HA.^{31–35} Increasing extracellular concentrations of UDP-GlcA and UDP-GlcNAc in the medium, both resulted in increased HA production in a *HAS2*-dependent manner (Figure 4A through 4D), especially UDP-GlcA, indicating that cellular availability of substrates determines HA production.

KLF2 Induces Intracellular UDP-Sugar Flux Through Regulating Glucose Usage

To test the critical cytosolic availability of UDP-GlcA and UDP-GlcNAc for HA biosynthesis in response to shear stress, we investigated substrate availability in relation to the endothelial metabolic state with *KLF2^{OE}*. Prolonged laminar shear repressed gene expression of the glycolytic activator *PFKFB3* through *KLF2* activation (Figure 5A

through 5C). Measuring the extracellular acidification rate, as an indicator of lactate production, showed reduced glucose-induced glycolysis and maximal glycolytic capacity, defined as extracellular acidification rate induced by the mitochondrial respiration blocker oligomycin to force the cells to rely more on glycolysis after *KLF2* overexpression of ECs (Figure VB in the [online-only Data Supplement](#)).

To test how this change in glycolytic rate influences the *HAS2* substrate availability, we used ¹³C labeled glucose in combination with NMR analysis to determine the intracellular fate of glucose-derived metabolites. *KLF2^{OE}* in ECs resulted in a reduced glucose uptake rate (Figure 5D) and lactate release rate (Figure 5E), consistent with the Seahorse data. The intracellular ¹³C-glucose amount was significantly increased on *KLF2^{OE}* (Figure 5F), however, without changes in relative ¹³C enrichment of intracellular glucose (Figure 5G, top row), which remains above 90%. This demonstrates that intracellular ¹²C-glucose was efficiently and proportionally replaced by ¹³C-glucose. When measuring subsequently the ¹³C-labeled glucose ring of the UDP-sugars which part will be incorporated into HA (Figure VC in the [online-only Data Supplement](#)), *KLF2^{OE}* increased the concentrations of UDP-Glc, UDP-GlcA, and UDP-GlcNAc (Figure 5H through 5J). Moreover, fractional ¹³C enrichment in the UDP-sugar glucose ring was also increased in *KLF2^{OE}* ECs while ¹³C labeled glucose was unchanged (Figure 5G), thus demonstrating induction of glucose flux into the UDP-sugars biosynthesis (Figure 5K). As expected, the fractional enrichment of the ¹³C-labeled ribose ring of the UDP-sugars, which will be released into the cytosol as UDP and potentially reused as synthetic precursor of UDP-sugars, did not change (Figure VD through VG in the [online-only Data Supplement](#)), suggesting the flux of glucose derived from UTP into UDP-sugars remains the same. In summary, reduced glycolysis on *KLF2^{OE}* in ECs resulted in a higher glucose flux into the UDP-GlcA and UDP-GlcNAc biosynthesis pathways (Figure 5K). In agreement, we observed reduced endothelial HA surface expression after knockdown of the key regulatory enzymes UDP-glucose pyrophosphorylase 2 (*UGP2*), UDP-glucose dehydrogenase (*UGDH*), or fructose amidotransferase 1 (*GFPT1*) in ECs exposed to laminar shear stress (Figure 5L and 5M) or in static culture without changing *HAS2* gene expression (Figure VIA through VIC).

Inhibition of Glycolysis by 3PO Increases HA Production

To confirm that the change of glycolytic rate influences HA biosynthesis, we used the pharmacological PFKFB3 inhibitor 3PO to decrease glycolysis in HUVECs. An increase of HA expression upon 3PO treatment was observed in ECs in static conditions in a *HAS2*-dependent manner (Figure 6A through 6C), while 3PO treatment did not change the *HAS2*- or

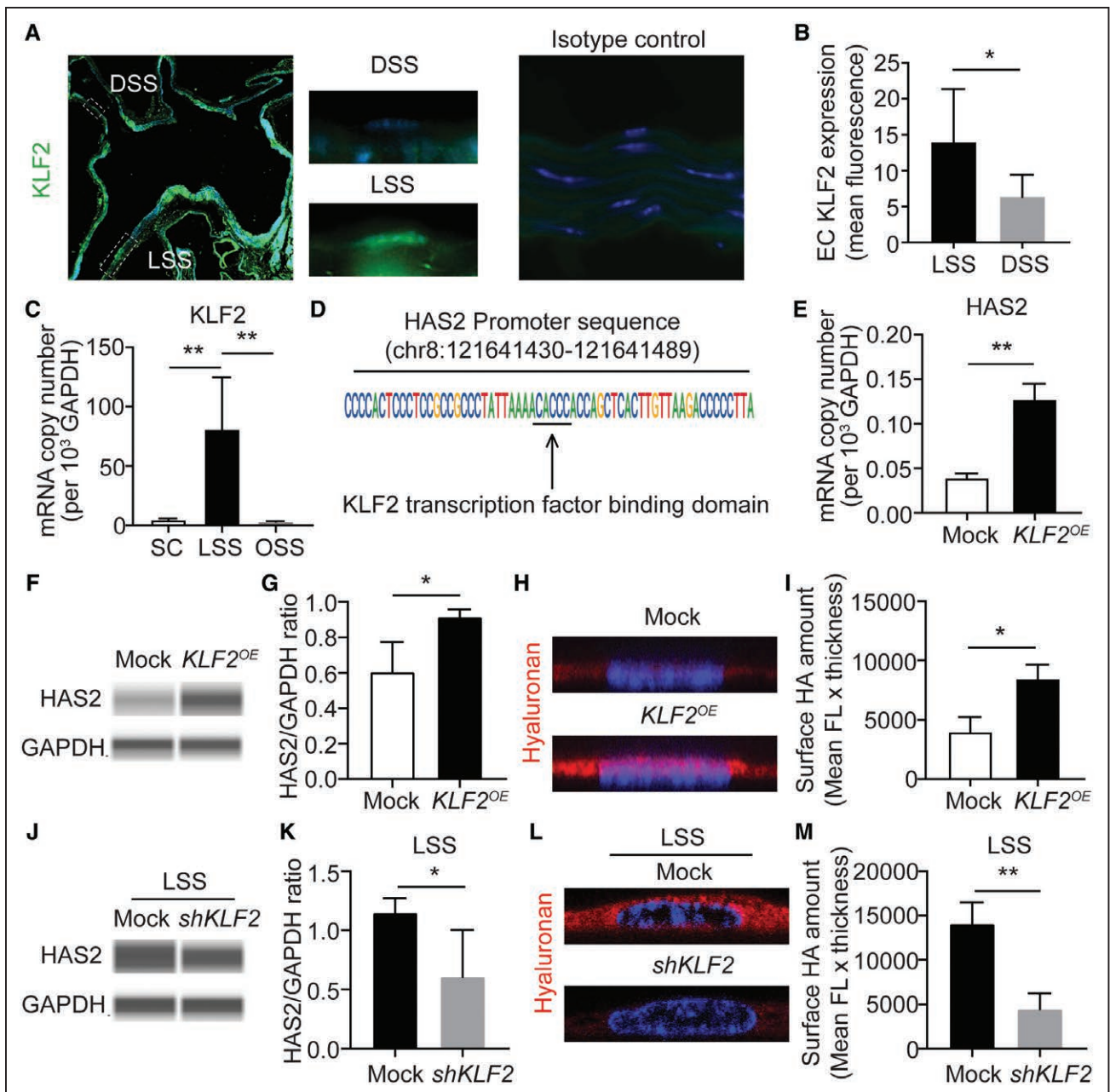


Figure 3. Laminar shear stress (LSS) induces hyaluronan (HA) production by increased KLF2 (Krüppel-like factor 2) expression and KLF2-mediated HAS2 (hyaluronan synthase 2) expression.

A, Representative images of KLF2 staining in the aortic arch region of *apoE*-KO mice on standard diet ($n=6$). Areas exposed to LSS or disturbed shear stress (DSS) are labeled, respectively. Rabbit IgG was used as an isotype control of KLF2 staining. **B**, Quantification of KLF2 protein expression. **C**, KLF2 mRNA expression in human umbilical vein endothelial cells (HUVECs) exposed to LSS or oscillatory shear stress (OSS). **D**, Highly conserved KLF2-binding domain CACCC as found in HAS2 promoter region. **E**, HAS2 mRNA expression in response to *KLF2* overexpression (*KLF2*^{OE}), normalized to 10^3 copies *GAPDH*. **F**, Representative WB images of endothelial HAS2 protein expression and (**G**) quantification in response to *KLF2*^{OE}. **H**, Representative confocal images of HA staining in HUVECs upon *KLF2*^{OE} with (**I**) quantification of surface HA. **J**, Representative WB images of endothelial HAS2 protein expression and (**K**) quantification after knockdown of *KLF2* (*shKLF2*) exposed to LSS. **L**, Representative confocal images of HA staining in HUVECs upon *shKLF2* exposed to LSS with (**M**) quantification of surface HA. All values are given as mean \pm SD of 3 to 7 independent experiments. Nonpaired 2-tailed Student *t* test and 1-way ANOVA followed by Tukey test were performed; * $P<0.05$, ** $P<0.01$.

3 expression itself (Figure 6D and 6E). Inhibition of glycolysis with a low dose of 2DG also increased HA production under static culture (Figure 6H). The same effect of 3PO treatment on HA production was

also shown in ECs exposed to oscillatory shear stress (Figure 6F). However, these effects were no longer detected when ECs were exposed to lamellar shear stress (10 dyne/cm²; Figure 6G).

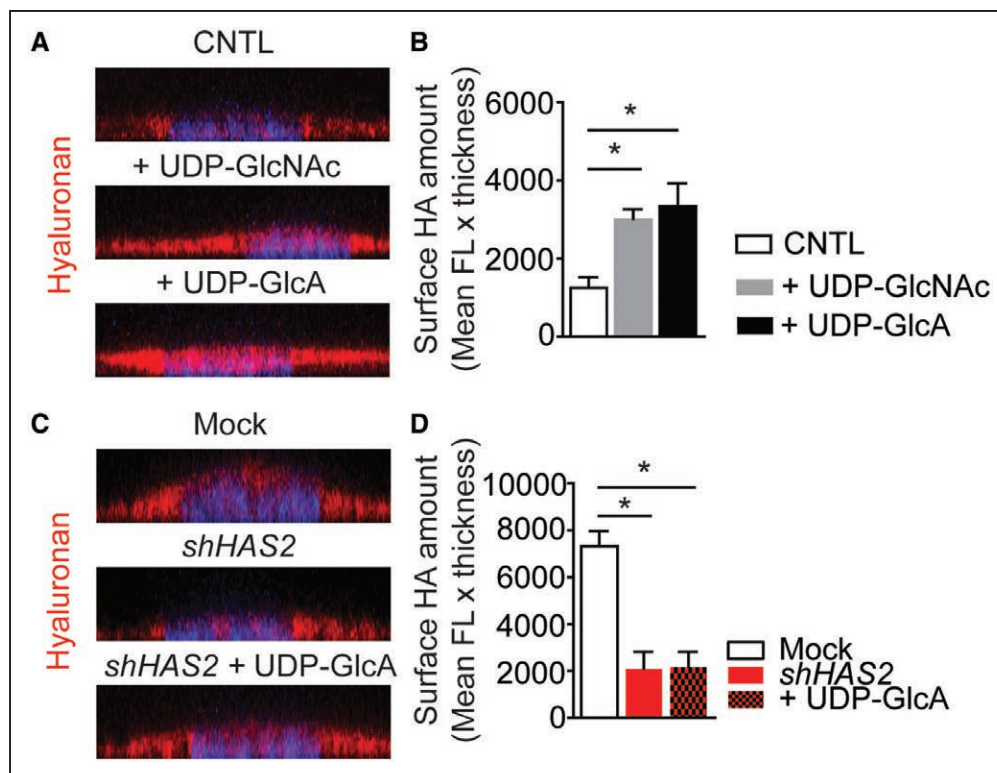


Figure 4. Hyaluronan (HA) synthesis by HAS2 (hyaluronan synthase 2) in endothelial cells is dependent on substrate availability.

A, Representative confocal images of HA staining and **(B)** quantification of endothelial surface HA on human umbilical vein endothelial cells (HUVECs) in the presence of 1 mmol/L UDP glucuronic acid (UDP-GlcA) or 1 mmol/L UDP-N-acetylglucosamine (UDP-GlcNAc) for 72 h. **C**, Representative confocal images of HA staining and **(D)** quantification of surface HA on HUVECs after knockdown of HAS2 (hyaluronan synthase 2; *shHAS2*), in presence of 1 mmol/L UDP-GlcA for 72 h. All values are given as mean \pm SD of 3 to 4 independent experiments. Nonpaired 2-tailed Student *t* test and 1-way ANOVA followed by Tukey test were performed; **P*<0.05.

DISCUSSION

The current study demonstrates how endothelial cell adaptation to alterations in shear stress through KLF2 is coupled to glycolytic flux (Figure 7A and 7B). We show that the endothelial glycolytic flux determines the availability of the cytosolic substrates UDP-GlcNAc and UDP-GlcA and that these are rate limiting to synthesis of the endothelial glycocalyx component HA. Consequently, KLF2-mediated suppression of glycolysis results in a thicker glycocalyx layer. Moreover, laminar shear is also accompanied by KLF2-dependent increase in synthesis and membrane localization of the HA-producing enzyme HAS2, which in quiescent EC seems to be the main HA producing enzyme.

The endothelial glycocalyx is critically involved in vascular integrity and homeostasis. Loss of this structure is associated with endothelial activation and dysfunction.^{36–38} HA in the glycocalyx has also been demonstrated to modulate inflammatory processes. The HMW form of HA possesses anti-inflammatory, anti-angiogenic, and immunosuppressive properties and protects cells from injury, and leukocyte adhesion.³⁹ In part, this is related to its gel-like physical properties that preclude direct contact of leukocytes with the endothelial surface. In addition, HA can modulate growth factor and chemokine gradients at the endothelial surface.

For example, binding of TNF (tumor necrosis factor)-stimulated gene 6 to HA inhibits chemokine-stimulated trans-endothelial migration of neutrophils via a direct interaction between TNF (tumor necrosis factor)-stimulated gene 6 and the glycosaminoglycan-binding site of CXCL8.⁴⁰ HA was also shown to mediate angiotensin 1 binding to its endothelial TIE2 receptor, thus constituting a cell surface matrix that regulates EC-pericyte cross communication.⁴¹ We recently corroborated the *in vivo* relevance of HA for endothelial glycocalyx function using an inducible endothelial deletion mouse model of *Has2*. Gene inactivation resulted in loss of glycocalyx structure, capillary destabilization, loss of endothelial barrier function and endothelial activation, and consequently in organ damage.⁴¹

Endothelial adaptation to shear is known to be a biphasic process.^{42–44} In the early phase (first hours), inflammatory signaling dominates and result in endothelial cell activation.^{43,44} This inflammatory signaling may also activate HAS2 and HA synthesis.^{43–46} However, HA polymerization in these conditions may lead to HA cable formation and contribute to inflammatory vascular remodeling.²⁸ After days of sustained laminar shear, the endothelial cells become quiescent after downregulation of its inflammatory pathways (Figure III in the [online-only Data Supplement](#)). Interestingly, as we show, this is again a stimulus for

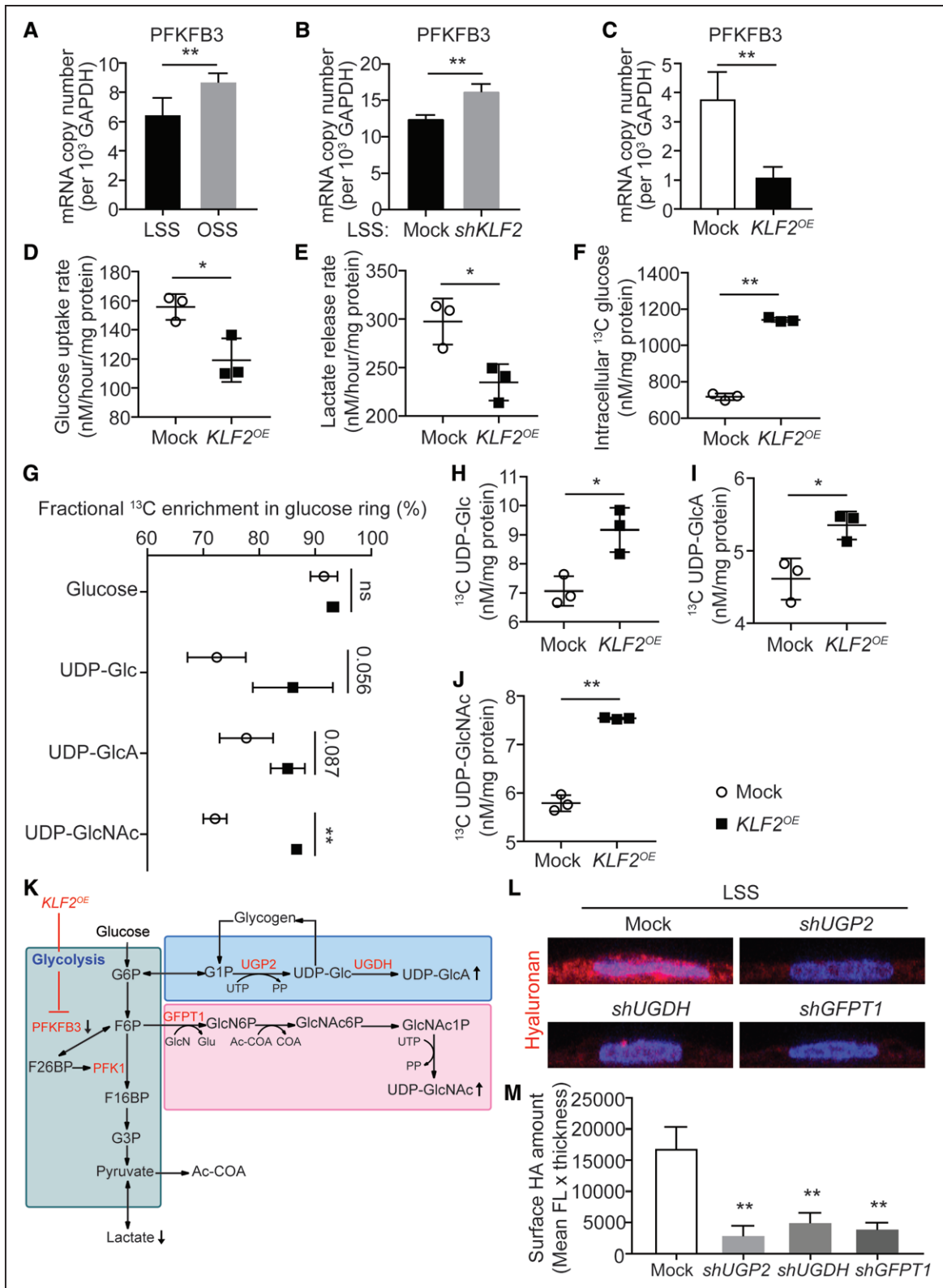


Figure 5. *KLF2* increases intracellular hyaluronan (HA) substrate availability and HA synthesis by shuttling UDP-sugar flux to the hexosamine- and glucuronic acid biosynthesis pathways.

A, PFKFB3 mRNA expression in human umbilical vein endothelial cells (HUVECs) exposed to laminar shear stress (LSS) or oscillatory shear stress (OSS). **B**, PFKFB3 mRNA expression in HUVECs on *shKLF2* exposed to LSS. **C**, PFKFB3 mRNA expression in HUVECs in response to *KLF2*^{OE}. Changes in intracellular and extracellular UDP-sugar metabolite concentrations are measured using NMR of ¹³C-glucose over ¹²C-glucose incorporation. **D**, Glucose uptake rate and **(E)** lactate release rate were quantified based on extracellular tracer concentrations before and after 24 h culture. **F**, Intracellular ¹³C glucose quantification change upon *KLF2*^{OE}. (Continued)

Figure 5 Continued. G, Enrichment analysis of the UDP-sugar ^{13}C labeled glucose ring as measure of ^{13}C flux change of UDP-sugars. Quantification of intracellular UDP-sugar metabolite measurements using the ^{13}C labeled glucose ring of **(H)** UDP glucose (UDP-Glc), **(I)** UDP glucuronic acid (UDP-GlcA), and **(J)** UDP-N-acetylglucosamine (UDP-GlcNAc). **K**, Pathway map of changed glucose usage through glycolysis and its side branches for UDP-sugars biosynthesis upon *KLF2*^{OE}. **L**, Representative confocal images of HA staining in HUVECs after knockdown of the key rate-limiting enzymes UDP-glucose pyrophosphorylase 2 (*shUGP2*), UDP-glucose dehydrogenase (*shUGDH*), or glutamine-fructose-6-phosphate transaminase 1 (*shGFPT1*), after 4 days of LSS exposure, and **(M)** quantification of surface HA. All values are given as mean \pm SD of 3 to 7 independent experiments. Nonpaired 2-tailed Student *t* test and 1-way ANOVA followed by Tukey test were performed; * P <0.05, ** P <0.01.

HA synthesis. This time it is KLF2 mediated, where HAS2 translocation and metabolic availability of the UDP-sugars that serve as substrate for HA polymerization are coregulated. We show that this coregulation is a critical step to endothelial glycolyx presence and function.

Part of the loss of endothelial glycolyx in conditions such as diabetes mellitus and cancer may be explained by increased activity of glycolyx degrading enzymes such as heparanase and hyaluronidase.⁴⁷ However, it must be assumed that glycolyx thickness is the resultant of synthesis and degradation. While the synthesis of heparan sulfate and chondroitin sulfate occurs in the Golgi, HA is synthesized directly at the plasma membrane from its precursor molecules, rendering its synthesis dependent on substrate availability, as indeed is shown in the current study. We recently demonstrated, using an inducible endothelial specific deletion of *has2* in mice, that loss of HA from the endothelial glycolyx results in collapse of the glycolyx, capillary destabilization, and loss of endothelial barrier function.⁴¹ It is therefore of interest therapeutically that cytosolic HA substrate availability can be increased by

slowing down endothelial glycolysis as well as by increasing the extracellular concentrations of these substrates. Apart from the shear-KLF2 pathway, which has previously been shown to inhibit the key glycolysis regulator PFKFB3,⁸ direct pharmacological inhibition of PFKFB3 has also been shown to be possible.⁴⁸ In the current study, we confirm that the PFKFB3 inhibitor 3PO can restore loss of endothelial HA during oscillatory flow.

In mammalian cells, the 3 HAS isoenzymes (HAS1, HAS2, and HAS3) differ in distribution and enzyme properties and in response to different stimuli.^{5,6,49} Among the 3 HASs, HAS1 expression is the lowest in healthy cells,⁵⁰ and it requires higher concentration of substrates for HA synthesis,⁵¹ while HAS3 was shown to produce shortest molecular weight HA.⁵ HAS2 is the most widespread isoform, which is also correlated to HA distribution.⁶ All 3 HASs have been shown to produce extracellular HA on the membrane, while HAS1 also produces intracellular HA.⁵⁰ We show that in endothelial cells HAS2 is the main enzyme to produce surface HA. HAS2 can be rapidly mobilized and transported to the plasma membrane for activation upon

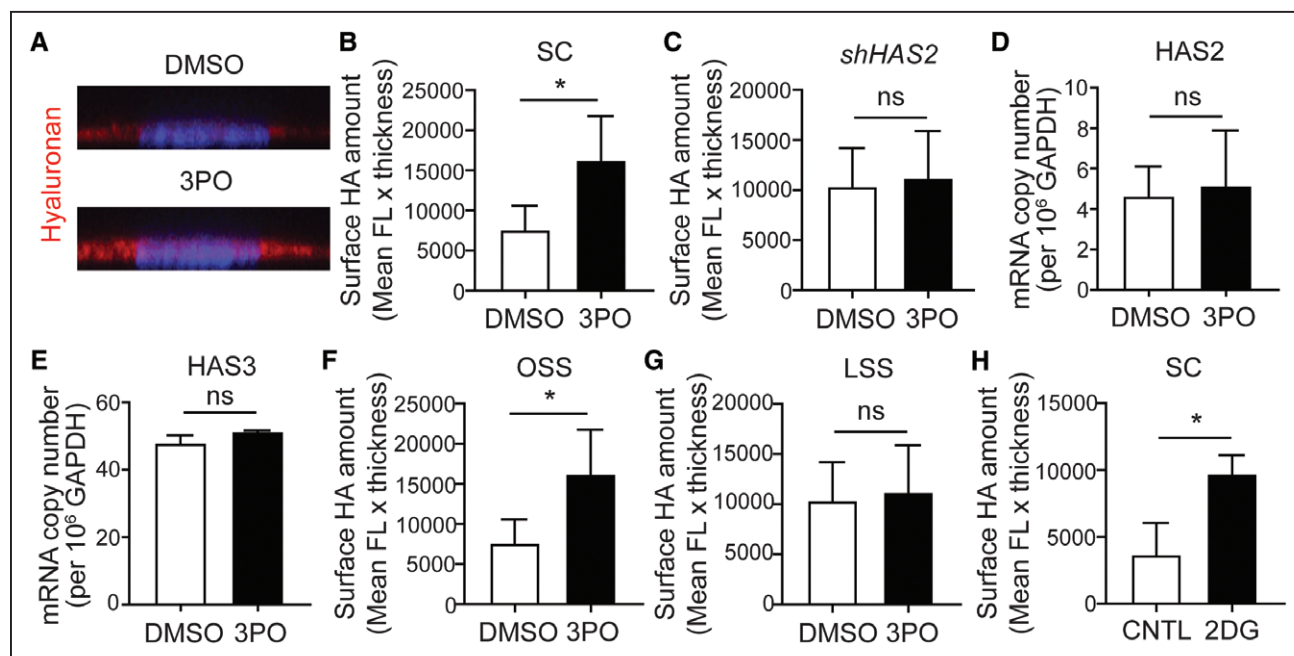


Figure 6. Inhibition of PFKFB3 by 3PO increases hyaluronan (HA) production.

A, Representative confocal images of HA staining of human umbilical vein endothelial cells (HUVECs) with PFKFB3 inhibitor (3PO) or DMSO as control under SC. Quantification of surface HA on HUVECs with 3PO treatment **(B)** under SC or **(C)** after knockdown of HAS2 (hyaluronan synthase 2) under SC. **D**, HAS2- and **(E)** HAS3 (hyaluronan synthase 3) mRNA expression in response to 3PO under SC, normalized to 10⁶ copies GAPDH. Quantification of surface HA on HUVECs with 3PO treatment **(F)** exposed to oscillatory shear stress (OSS) or **(G)** laminar shear stress (LSS). **H**, Quantification of surface HA on HUVECs with 2-deoxy-D-glucose (2DG) treatment under SC. All values are given as mean \pm SD of 3 to 4 independent experiments. Nonpaired 2-tailed Student *t* test was performed; * P <0.05.

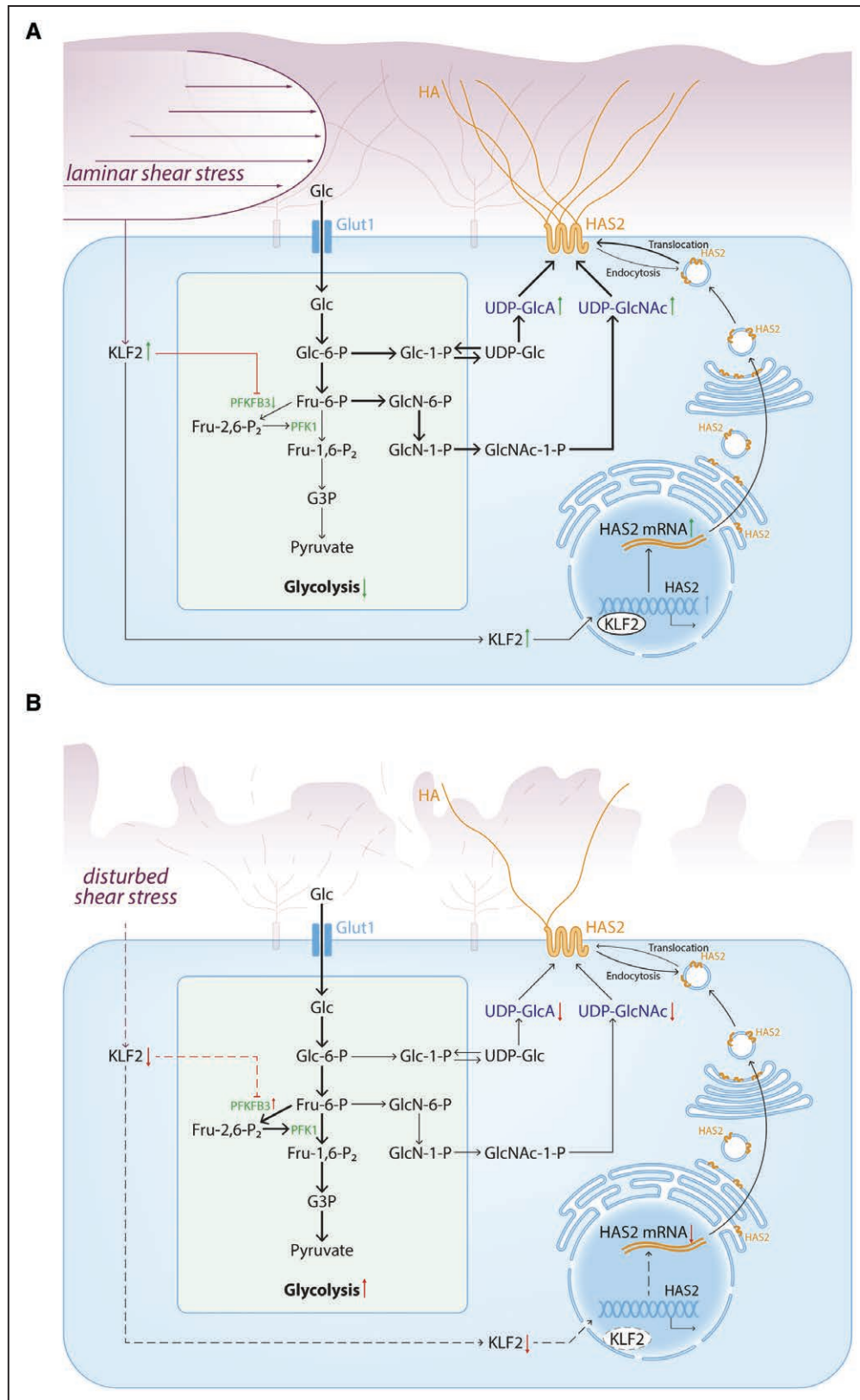


Figure 7. Schematic overview of the shear stress regulated endothelial hyaluronan production.

A, Laminar shear stress induces endothelial hyaluronan (HA) production through KLF2 (Krüppel-like factor 2) activation and subsequent inhibition of the glycolytic activator PFKFB3, which allows glucose intermediates to shuttle into the biosynthetic pathways of UDP glucuronic acid (UDP-GlcA) and UDP-N-acetylglucosamine (UDP-GlcNAc) and meanwhile increases surface HAS2 (hyaluronan synthase 2) presence through regulating HAS2 mRNA transcription and protein translocation. **B**, Disturbed shear stress reduces endothelial HA production by limiting both surface HAS2 enzyme and its substrates availability.

laminar shear.^{6,28} The exact mechanism of how shear also increases HAS2 protein concentrations still needs to be established but could be related to the fact that HAS2 has been shown to be stabilized by O-GlcNAcylation.⁵²

CRISPR-Cas9 has been used to insert exogenous sequences into specific genomic sites via homology directed repair.⁵³ Cas9-mediated protein tagging simplified experimental analysis of protein function. However, knock-in of fluorescent tags (ie, GFP or RFP [red fluorescent protein]) to proteins can change its normal behavior within the cell.⁵⁴ Here, we inserted a small TC-tag (Cys-Cys-Pro-Gly-Cys-Cys) into the C-terminal end of the *HAS2* gene, using a non-viral Cas9 ribonucleoprotein system in primary endothelial cells.⁵⁵ Once the nonfluorescent FIAH-EDT2 and ReAsH-EDT2 labeling reagents bind the TC-tag fused protein, the reagents will be converted to a highly fluorescent state.⁵⁶ We developed a genomic labeling technique of *HAS2* in primary endothelial cells that can be used to determine endogenous HAS2 expression and localization in live cells, and it also can be potentially applied to determine HAS2 protein stability and recycling capacity using time-lapse confocal microscopy.

In summary, we showed that quiescent endothelial cells, induced by prolonged laminar shear stress, presented a thicker glycocalyx HA on the surface through KLF2 regulated HAS2 expression and UDP-sugar availability. HAS2 was determined as the main HA synthase for HA in endothelial cells, regulated by UDP-GlcA. Endothelial cells need proper amount of HA to keep its integrity, which is likely determined by the metabolic state of endothelial cells, such as found under laminar shear stress.

ARTICLE INFORMATION

Received April 4, 2019; accepted November 26, 2019.

Affiliations

From the Division of Nephrology, Department of Internal Medicine (G.W., G.L.T., W.M.P.J.S., B.M.v.d.B., T.J.R.) and Department of Surgery (M.R.d.V.), The Einthoven Laboratory for Vascular and Regenerative Medicine, Leiden University Medical Center, the Netherlands; Center for Proteomics and Metabolomics, Leiden University Medical Center, the Netherlands (S.K., M.G.); Department of Oncology, Laboratory of Angiogenesis and Vascular Metabolism, KU Leuven, Vesalius Research Center, VIB, Belgium (P.C.); and Laboratory of Angiogenesis and Vascular Metabolism, Vesalius Research Center, VIB, Leuven, Belgium (P.C.).

Acknowledgments

We thank Cleveland Clinics to provide the online protocol for HA size analysis (NHLBI # PO1HL107147). We thank Dr William C. Aird (Center for Vascular Biology Research, Division of Molecular and Vascular Medicine, Beth Israel Deaconess Medical Center, Boston, MA) for allowing to construct the following shUGP2, shUGDH, and shGFPT1 vectors, Dr McCarthy (Laboratory Medicine and Pathology, University of Minnesota, Minneapolis, MN) for providing HAS2 gene construct, Dr Curiel (Division of Human Gene Therapy, Departments of Medicine, Pathology and Surgery, and the Gene Therapy Center, University of Alabama at Birmingham, Birmingham, AL) for providing the adenoviral vector Ad5CMV-HAS2 and Ad5CMV-Luciferase constructs, and Dr Kappler (Institut für Biochemie und Molekularbiologie, Universität Bonn, Germany) for providing the neurocan-eGFP construct.

Sources of Funding

We gratefully acknowledge the financial Support by the Dutch Kidney Foundation (grant C08.2265) and the China Scholarship Council grant to Gangqi Wang (CSC no. 201406170050).

Disclosures

None.

REFERENCES

1. Reitsma S, Slaaf DW, Vink H, van Zandvoort MA, oude Egbrink MG. The endothelial glycocalyx: composition, functions, and visualization. *Pflugers Arch*. 2007;454:345–359. doi: 10.1007/s00424-007-0212-8
2. Weinbaum S, Tarbell JM, Damiano ER. The structure and function of the endothelial glycocalyx layer. *Annu Rev Biomed Eng*. 2007;9:121–167. doi: 10.1146/annurev.bioeng.9.060906.151959
3. Lewis JC, Taylor RG, Jones ND, St Clair RW, Cornhill JF. Endothelial surface characteristics in pigeon coronary artery atherosclerosis. I. Cellular alterations during the initial stages of dietary cholesterol challenge. *Lab Invest*. 1982;46:123–138.
4. van den Berg BM, Spaan JA, Rolf TM, Vink H. Atherogenic region and diet diminish glycocalyx dimension and increase intima-to-media ratios at murine carotid artery bifurcation. *Am J Physiol Heart Circ Physiol*. 2006;290:H915–H920. doi: 10.1152/ajpheart.00051.2005
5. Itano N, Sawai T, Yoshida M, Lenas P, Yamada Y, Imagawa M, Shinomura T, Hamaguchi M, Yoshida Y, Ohnuki Y, et al. Three isoforms of mammalian hyaluronan synthases have distinct enzymatic properties. *J Biol Chem*. 1999;274:25085–25092. doi: 10.1074/jbc.274.35.25085
6. Törrönen K, Nikunen K, Kärrä R, Tammi M, Tammi R, Rilla K. Tissue distribution and subcellular localization of hyaluronan synthase isoenzymes. *Histochem Cell Biol*. 2014;141:17–31. doi: 10.1007/s00418-013-1143-4
7. Moretto P, Karousou E, Viola M, Caon I, D'Angelo ML, De Luca G, Passi A, Vigetti D. Regulation of hyaluronan synthesis in vascular diseases and diabetes. *J Diabetes Res*. 2015;2015:167283. doi: 10.1155/2015/167283
8. Doddaballapur A, Michalik KM, Manavski Y, Lucas T, Houtkooper RH, You X, Chen W, Zeiher AM, Potente M, Dimmeler S, et al. Laminar shear stress inhibits endothelial cell metabolism via KLF2-mediated repression of PFKFB3. *Arterioscler Thromb Vasc Biol*. 2015;35:137–145. doi: 10.1161/ATVBAHA.114.304277
9. Meuwese MC, Broekhuizen LN, Kuikhoven M, Heeneman S, Lutgens E, Gijbels MJ, Nieuwdorp M, Peutz CJ, Stroes ES, Vink H, et al. Endothelial surface layer degradation by chronic hyaluronidase infusion induces proteinuria in apolipoprotein E-deficient mice. *PLoS One*. 2010;5:e14262. doi: 10.1371/journal.pone.0014262
10. Huxley VH, Wang J, Whitt SP. Sexual dimorphism in the permeability response of coronary microvessels to adenosine. *Am J Physiol Heart Circ Physiol*. 2005;288:H2006–H2013. doi: 10.1152/ajpheart.01007.2004
11. Jaffe EA, Nachman RL, Becker CG, Minick CR. Culture of human endothelial cells derived from umbilical veins. Identification by morphologic and immunologic criteria. *J Clin Invest*. 1973;52:2745–2756. doi: 10.1172/JCI107470
12. Cheng C, Helderma F, Tempel D, Segers D, Hierck B, Poelmann R, van Tol A, Duncker DJ, Robbers-Visser D, Ursem NT, et al. Large variations in absolute wall shear stress levels within one species and between species. *Atherosclerosis*. 2007;195:225–235. doi: 10.1016/j.atherosclerosis.2006.11.019
13. Malek AM, Alper SL, Izumo S. Hemodynamic shear stress and its role in atherosclerosis. *JAMA*. 1999;282:2035–2042. doi: 10.1001/jama.282.21.2035
14. Hosoya T, Maruyama A, Kang MI, Kawatani Y, Shibata T, Uchida K, Warabi E, Noguchi N, Itoh K, Yamamoto M. Differential responses of the Nrf2-Keap1 system to laminar and oscillatory shear stresses in endothelial cells. *J Biol Chem*. 2005;280:27244–27250. doi: 10.1074/jbc.M502551200
15. Chatzizisis YS, Coskun AU, Jonas M, Edelman ER, Feldman CL, Stone PH. Role of endothelial shear stress in the natural history of coronary atherosclerosis and vascular remodeling: molecular, cellular, and vascular behavior. *J Am Coll Cardiol*. 2007;49:2379–2393. doi: 10.1016/j.jacc.2007.02.059
16. Mahler GJ, Frenzl CM, Cao Q, Butcher JT. Effects of shear stress pattern and magnitude on mesenchymal transformation and invasion of aortic valve endothelial cells. *Biotechnol Bioeng*. 2014;111:2326–2337. doi: 10.1002/bit.25291
17. Sorop O, Spaan JA, Sweeney TE, VanBavel E. Effect of steady versus oscillating flow on porcine coronary arterioles: involvement of NO and superoxide anion. *Circ Res*. 2003;92:1344–1351. doi: 10.1161/01.RES.0000078604.47063.2B
18. Timmins LH, Molony DS, Eshtehardi P, McDaniel MC, Oshinski JN, Giddens DP, Samady H. Oscillatory wall shear stress is a dominant flow characteristic affecting lesion progression patterns and plaque vulnerability in patients with coronary artery disease. *J R Soc Interface*. 2017;14:20160972. doi: 10.1098/rsif.2016.0972
19. Zhang H, Baader SL, Sixt M, Kappler J, Rauch U. Neurocan-GFP fusion protein: a new approach to detect hyaluronan on tissue sections and

- living cells. *J Histochem Cytochem*. 2004;52:915–922. doi: 10.1369/jhc.3A6221.2004
20. Boels MG, Avramut MC, Koudijs A, Dane MJ, Lee DH, van der Vlag J, Koster AJ, van Zonneveld AJ, van Faassen E, Gröne HJ, et al. Atrasentan reduces albuminuria by restoring the glomerular endothelial glycocalyx barrier in diabetic nephropathy. *Diabetes*. 2016;65:2429–2439. doi: 10.2337/db15-1413
 21. van der Veer EP, de Bruin RG, Kraaijeveld AO, de Vries MR, Bot I, Pera T, Segers FM, Trompet S, van Gils JM, Roeten MK, et al. Quaking, an RNA-binding protein, is a critical regulator of vascular smooth muscle cell phenotype. *Circ Res*. 2013;113:1065–1075. doi: 10.1161/CIRCRESAHA.113.301302
 22. Simpson MA, Wilson CM, Furcht LT, Spicer AP, Oegema TR Jr, McCarthy JB. Manipulation of hyaluronan synthase expression in prostate adenocarcinoma cells alters pericellular matrix retention and adhesion to bone marrow endothelial cells. *J Biol Chem*. 2002;277:10050–10057. doi: 10.1074/jbc.M110069200
 23. Wu H, Dmitriev I, Kashentseva E, Seki T, Wang M, Curiel DT. Construction and characterization of adenovirus serotype 5 packaged by serotype 3 hexon. *J Virol*. 2002;76:12775–12782. doi: 10.1128/jvi.76.24.12775-12782.2002
 24. Kostidis S, Addie RD, Morreau H, Mayboroda OA, Giera M. Quantitative NMR analysis of intra- and extracellular metabolism of mammalian cells: a tutorial. *Anal Chim Acta*. 2017;980:1–24. doi: 10.1016/j.aca.2017.05.011
 25. Vinaixa M, Rodriguez MA, Aivio S, Capellades J, Gomez J, Canyellas N, Stracker TH, Yanes O. Positional enrichment by proton analysis (pepa): a one-dimensional (1) h-nmr approach for (13) c stable isotope tracer studies in metabolomics. *Angew Chem Int Ed Engl*. 2017;56:3531–3535. doi: 10.1002/anie.201611347
 26. Dekker RJ, van Soest S, Fontijn RD, Salamanca S, de Groot PG, VanBavel E, Pannekoek H, Horrevoets AJ. Prolonged fluid shear stress induces a distinct set of endothelial cell genes, most specifically lung Kruppel-like factor (KLF2). *Blood*. 2002;100:1689–1698. doi: 10.1182/blood-2002-01-0046
 27. Cyphert JM, Trempus CS, Garantzios S. Size matters: molecular weight specificity of hyaluronan effects in cell biology. *Int J Cell Biol*. 2015;2015:563818. doi: 10.1155/2015/563818
 28. Hascall VC, Majors AK, De La Motte CA, Evanko SP, Wang A, Drabza JA, Strong SA, Wight TN. Intracellular hyaluronan: a new frontier for inflammation? *Biochim Biophys Acta*. 2004;1673:3–12. doi: 10.1016/j.bbagen.2004.02.013
 29. Miller IJ, Bieker JJ. A novel, erythroid cell-specific murine transcription factor that binds to the CACCC element and is related to the Kruppel family of nuclear proteins. *Mol Cell Biol*. 1993;13:2776–2786. doi: 10.1128/mcb.13.5.2776
 30. Zhang P, Basu P, Redmond LC, Morris PE, Rupon JW, Ginder GD, Lloyd JA. A functional screen for kruppel-like factors that regulate the human gamma-globin gene through the cacc promoter element. *Blood Cell Mol Dis*. 2005;35:227–235. doi: 10.1016/j.bcmd.2005.04.009
 31. Vigetti D, Viola M, Karousou E, De Luca G, Passi A. Metabolic control of hyaluronan synthases. *Matrix Biol*. 2014;35:8–13. doi: 10.1016/j.matbio.2013.10.002
 32. Vigetti D, Ori M, Viola M, Genasetti A, Karousou E, Rizzi M, Pallotti F, Nardi I, Hascall VC, De Luca G, et al. Molecular cloning and characterization of UDP-glucose dehydrogenase from the amphibian *Xenopus laevis* and its involvement in hyaluronan synthesis. *J Biol Chem*. 2006;281:8254–8263. doi: 10.1074/jbc.M508516200
 33. Baggenstoss BA, Harris EN, Washburn JL, Medina AP, Nguyen L, Weigel PH. Hyaluronan synthase control of synthesis rate and hyaluronan product size are independent functions differentially affected by mutations in a conserved tandem B-X7-B motif. *Glycobiology*. 2017;27:154–164. doi: 10.1093/glycob/cww089
 34. Viola M, Karousou E, D'Angelo ML, Caon I, De Luca G, Passi A, Vigetti D. Regulated hyaluronan synthesis by vascular cells. *Int J Cell Biol*. 2015;2015:208303. doi: 10.1155/2015/208303
 35. Slawson C, Copeland RJ, Hart GW. O-GlcNAc signaling: a metabolic link between diabetes and cancer? *Trends Biochem Sci*. 2010;35:547–555. doi: 10.1016/j.tibs.2010.04.005
 36. Tarbell JM, Cancel LM. The glycocalyx and its significance in human medicine. *J Intern Med*. 2016;280:97–113. doi: 10.1111/joim.12465
 37. Broekhuizen LN, Mooij HL, Kastelein JJ, Stroes ES, Vink H, Nieuwdorp M. Endothelial glycocalyx as potential diagnostic and therapeutic target in cardiovascular disease. *Curr Opin Lipidol*. 2009;20:57–62. doi: 10.1097/MOL.0b013e328321b587
 38. Lee DH, Dane MJ, van den Berg BM, Boels MG, van Teeffelen JW, de Mutser R, den Heijer M, Rosendaal FR, van der Vlag J, van Zonneveld AJ, et al; NEO study group. Deeper penetration of erythrocytes into the endothelial glycocalyx is associated with impaired microvascular perfusion. *PLoS One*. 2014;9:e96477. doi: 10.1371/journal.pone.0096477
 39. Yung S, Thomas GJ, Davies M. Induction of hyaluronan metabolism after mechanical injury of human peritoneal mesothelial cells *in vitro*. *Kidney Int*. 2000;58:1953–1962. doi: 10.1111/j.1523-1755.2000.00367.x
 40. Dyer DP, Thomson JM, Hermant A, Jowitt TA, Handel TM, Proudfoot AE, Day AJ, Milner CM. TSG-6 inhibits neutrophil migration via direct interaction with the chemokine CXCL8. *J Immunol*. 2014;192:2177–2185. doi: 10.4049/jimmunol.1300194
 41. van den Berg BM, Wang G, Boels MGS, Avramut MC, Jansen E, Sol W, Lebrin F, Jan van Zonneveld A, de Koning EJP, Vink H, et al. Glomerular function and structural integrity depend on hyaluronan synthesis by glomerular endothelium. *J Am Soc Nephrol*. 2019;30:1886–1897. doi: 10.1681/ASN.2019020192
 42. Shyy YJ, Hsieh HJ, Usami S, Chien S. Fluid shear stress induces a biphasic response of human monocyte chemotactic protein 1 gene expression in vascular endothelium. *Proc Natl Acad Sci U S A*. 1994;91:4678–4682. doi: 10.1073/pnas.91.11.4678
 43. Tzima E, Del Pozo MA, Kiosses WB, Mohamed SA, Li S, Chien S, Schwartz MA. Activation of Rac1 by shear stress in endothelial cells mediates both cytoskeletal reorganization and effects on gene expression. *EMBO J*. 2002;21:6791–6800. doi: 10.1093/emboj/cdf688
 44. Tzima E, Irani-Tehrani M, Kiosses WB, Dejana E, Schultz DA, Engelhardt B, Cao G, DeLisser H, Schwartz MA. A mechanosensory complex that mediates the endothelial cell response to fluid shear stress. *Nature*. 2005;437:426–431. doi: 10.1038/nature03952
 45. Vigetti D, Genasetti A, Karousou E, Viola M, Moretto P, Clerici M, Deleonibus S, De Luca G, Hascall VC, Passi A. Proinflammatory cytokines induce hyaluronan synthesis and monocyte adhesion in human endothelial cells through hyaluronan synthase 2 (HAS2) and the nuclear factor-kappaB (NF-kappaB) pathway. *J Biol Chem*. 2010;285:24639–24645. doi: 10.1074/jbc.M110.134536
 46. Maroski J, Vorderwülbecke BJ, Fiedorowicz K, Da Silva-Azevedo L, Siegel G, Marki A, Pries AR, Zakrzewicz A. Shear stress increases endothelial hyaluronan synthase 2 and hyaluronan synthesis especially in regard to an atheroprotective flow profile. *Exp Physiol*. 2011;96:977–986. doi: 10.1113/expphysiol.2010.056051
 47. Rabelink TJ, van den Berg BM, Garsen M, Wang G, Elkin M, van der Vlag J. Heparanase: roles in cell survival, extracellular matrix remodelling and the development of kidney disease. *Nat Rev Nephrol*. 2017;13:201–212. doi: 10.1038/nrneph.2017.6
 48. Cantelmo AR, Conradi LC, Brajic A, Goveia J, Kalucka J, Pircher A, Chaturvedi P, Hol J, Thienpont B, Teuwen LA, et al. Inhibition of the glycolytic activator PFKFB3 in endothelium induces tumor vessel normalization, impairs metastasis, and improves chemotherapy. *Cancer Cell*. 2016;30:968–985. doi: 10.1016/j.ccell.2016.10.006
 49. Jacobson A, Brinck J, Briskin MJ, Spicer AP, Heldin P. Expression of human hyaluronan synthases in response to external stimuli. *Biochem J*. 2000;348(pt 1):29–35.
 50. Siiskonen H, Oikari S, Pasonen-Seppänen S, Rilla K. Hyaluronan synthase 1: a mysterious enzyme with unexpected functions. *Front Immunol*. 2015;6:43. doi: 10.3389/fimmu.2015.00043
 51. Rilla K, Oikari S, Jokela TA, Hyttinen JM, Kärnä R, Tammi RH, Tammi MI. Hyaluronan synthase 1 (HAS1) requires higher cellular UDP-GlcNAc concentration than HAS2 and HAS3. *J Biol Chem*. 2013;288:5973–5983. doi: 10.1074/jbc.M112.443879
 52. Vigetti D, Deleonibus S, Moretto P, Karousou E, Viola M, Bartolini B, Hascall VC, Tammi M, De Luca G, Passi A. Role of UDP-N-acetylglucosamine (GlcNAc) and O-GlcNAcylation of hyaluronan synthase 2 in the control of chondroitin sulfate and hyaluronan synthesis. *J Biol Chem*. 2012;287:35544–35555. doi: 10.1074/jbc.M112.402347
 53. Ran FA, Hsu PD, Wright J, Agarwala V, Scott DA, Zhang F. Genome engineering using the CRISPR-Cas9 system. *Nat Protoc*. 2013;8:2281–2308. doi: 10.1038/nprot.2013.143
 54. Crivat G, Taraska JW. Imaging proteins inside cells with fluorescent tags. *Trends Biotechnol*. 2012;30:8–16. doi: 10.1016/j.tibtech.2011.08.002
 55. Dewari PS, Southgate B, McCarten K, Monogarov G, O'Duibhir E, Quinn N, Tyrer A, Leitner MC, Plumb C, Kalantzaki M, et al. An efficient and scalable pipeline for epitope tagging in mammalian stem cells using cas9 ribonucleoprotein. *Elife*. 2018;7:e35069. doi: 10.7554/eLife.35069
 56. Hoffmann C, Gaietta G, Zürn A, Adams SR, Terrillon S, Ellisman MH, Tsien RY, Lohse MJ. Fluorescent labeling of tetracysteine-tagged proteins in intact cells. *Nat Protoc*. 2010;5:1666–1677. doi: 10.1038/nprot.2010.129